Synthesis and characterization of (3-aminopropyl) triethoxysilane (APTES) functionalized zeolite AlPO-18

To cite this article: L D Anbealagan *et al* 2021 *IOP Conf. Ser.: Mater. Sci. Eng.* **1195** 012047

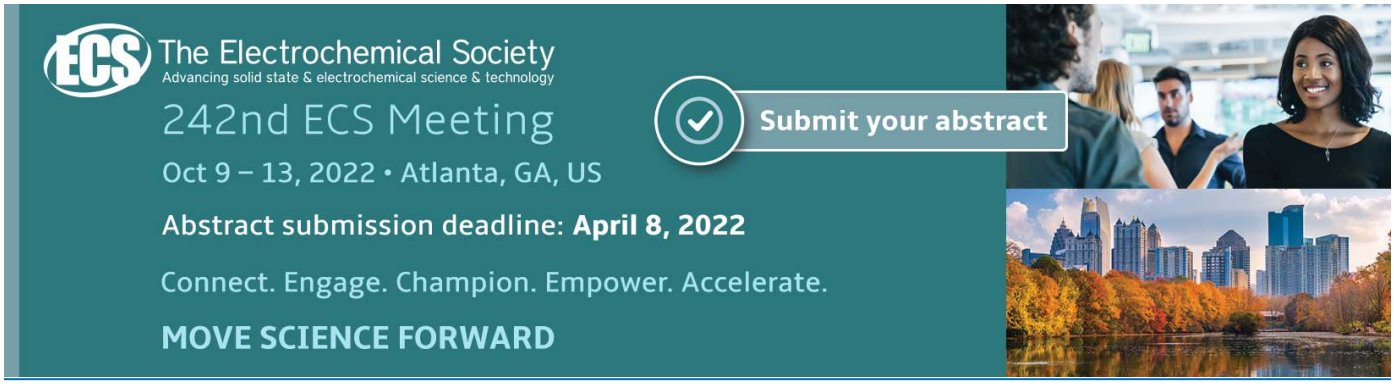

Synthesis and characterization of (3-aminopropyl) triethoxysilane (APTES) functionalized zeolite AlPO-18

L D Anbealagan[1,2], T L Chew[1,2], Y F Yeong[1,2], Z A Jawad[3] and C D Ho[4]

[1] Department of Chemical Engineering, Faculty of Engineering, University Teknologi PETRONAS, 32610 Seri Iskandar, Perak, Malaysia
[2] CO_2 Research Centre (CO_2RES), Institute Contaminant Management, University Teknologi PETRONAS, 32610 Seri Iskandar, Perak, Malaysia
[3] Department of Chemical Engineering, College of Engineering, Qatar University, P.O. Box: 2713, Doha, Qatar
[4] Department of Chemical and Materials Engineering, Tamkang University, New Taipei City 25137, Taiwan

Email: lanisha_19000945@utp.edu.my, thiamleng.chew@utp.edu.my

Abstract. Over the years, functionalization of zeolite is gaining popularity among researchers to further modify the properties of the zeolite for wide applications. The procedure of functionalization is crucial to ensure that the framework and structure of the zeolite would not be destroyed by the functionalization process. In this work, zeolite AlPO-18 was synthesized via hydrothermal synthesis method and functionalized by (3-Aminopropyl) triethoxysilane (APTES). The effect of the APTES functionalization on zeolite AlPO-18 was investigated in this work. Both unfunctionalized and silane-functionalized zeolite AlPO-18 were characterized using Fourier-transform infrared spectroscopy (FT-IR), X-ray diffraction (XRD), and Thermogravimetric analysis (TGA) for their properties. The morphology and the composition of the elements present in zeolite AlPO-18 and zeolite NH_2-AlPO-18 were examined using Field Emission Scanning Electron Microscopy (FESEM) and Energy-Dispersive spectroscopy (EDX) respectively. The XRD pattern of NH_2-AlPO-18 was similar to that of zeolite AlPO-18, however, the intensity of the peaks was lower compared to zeolite AlPO-18. Based on the FTIR spectra, the presence of N-H stretching and bending vibration band of aminosilane were observed in the NH_2-AlPO-18 sample. According to FESEM images, the morphology of NH_2-AlPO-18 was comparable to that of zeolite AlPO-18 even after functionalization, proving that functionalization of aminosilane on zeolite does not affect on the zeolite structure. Besides that, EDX proves the presence of 3.02 % of element N in the NH_2-AlPO-18 sample which is absent in the zeolite AlPO-18 sample. All of the characterizations evinced the presence of aminosilane, APTES in the NH_2-AlPO-18 sample.

1. Introduction

Zeolites are crystalline aluminosilicates with a well-defined pore framework made from interlinked tetrahedra of SiO_4 and AlO_4 [1]. Currently, there are more than 200 types of zeolites have been documented, such as zeolite T, SAPO-34, DDR, SSZ-13, Si-CHA, and AlPO-18 [2]. Zeolites can be differentiated based on their crystal structure and framework. It exhibits a well-defined and uniform pore size with a large surface area and high porosity. Zeolites can be categorized based on the pore size

such as small pore (6-, 8- and 9- membered ring), medium pore (10- membered ring), and large pore (12- membered ring) [3]. Zeolites have been used in various industrial applications such as adsorption, catalysis, and gas separations due to their intrinsic characteristics such as high chemical, thermal and mechanical stabilities [3].

Zeolite AlPO-18 is a type of zeolite that is gaining favor among researchers because of its small pore structure. Zeolite AlPO-18 is a type of zeolite that is made up of aluminum, phosphorus, and oxygen and consists of 3D structured pores possessing 8-membered rings with a pore size of 3.8 Å. The framework density of AlPO-18 of 15.1 T/nm^3 is the lowest among the aluminophosphate family. Zeolite AlPO-18 also has a low hydrophilicity nature. The low framework density, as well as the low hydrophilicity properties, are the predominant feature of AlPO [4]. It can be synthesized at a moderate synthesis temperature and a short synthesis duration. Zeolite AlPO-18 has been researched for applications including gas separation. It is remained an interest among researchers to explore approaches in modifying or improving the properties of zeolite AlPO-18 to be suitably applied at different applications.

Functionalization of zeolites using different types of silane coupling agents is among the effective technique used to modify the zeolite properties for wide applications [5–9]. The most commonly used silane coupling agents are (γ-aminopropyl)-triethoxysilane (APTES), 3-aminopropylmethyldiethoxysilane (APMDES) and (γ-aminopropyl)-diethoxymethylsilane (APDEMS) [10-15]. It contains two types of reactive functional groups including organic and inorganic groups. R – $(CH_2)_n$ – Si – X_{4-n} is the typical structure of silane coupling agents, where R represents the organo-functional group (amine, methacryloxy or, epoxy) and X represents the hydrolysable group (methoxy, ethoxy, or acetoxy) [16, 17]. During the functionalization process, the hydroxyl group on the inorganic filler surface reacts with the silane [18, 19].

In the present work, APTES has been chosen to be used as the silane coupling agent as it has been extensively used for a wide range of applications and it could also be considered as one of the less expensive silane coupling agents compared to the others [20–28]. APTES consists of an amine group (NH_2) and three ethoxy groups that can be adhered to the zeolite surface [22, 29]. Figure 1 depicts the schematic illustration for zeolite AlPO-18 functionalization using an APTES silane coupling agent. The novelty of the work is the functionalization of zeolite AlPO-18 using APTES and investigating the effect of the functionalization on the zeolite. Both unfunctionalized and silane-functionalized zeolite AlPO-18 were characterized using XRD, FT-IR, TGA, and FESEM. To date, there are no research works reported on the functionalization of zeolite AlPO-18 by using APTES.

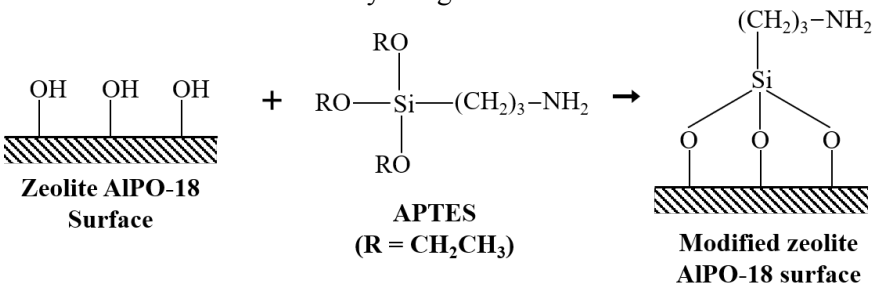

Figure 1. Schematic illustration for aminosilane functionalization of zeolite AlPO-18.

2. Materials and experimental procedures

2.1. Materials

Aluminium isopropoxide (98 %, Sigma Aldrich), tetramethylammonium hydroxide (TEAOH) (35 % in water, Sigma Aldrich), phosphoric acid (H_3PO_4) (85 wt % aqueous solution, Sigma Aldrich), and deionized water (DI water) were used for zeolite AlPO-18 synthesis. The silane coupling agent, (3-aminopropyl)-triethoxysilane (APTES) (99 %, Sigma Aldrich) was used to modify zeolite. Toluene (> 99.9 %) and ethanol (> 99.9 %) were supplied by Merck Co. All the chemicals were used as received.

2.2. Synthesis of zeolite AlPO-18

Zeolite AlPO-18 was synthesized via hydrothermal synthesis method by following the literature reported [30, 31]. A precursor solution with a molar composition of 1.0 Al_2O_3: 3.16 P_2O_5: 6.32 TEAOH: 186 H_2O was prepared. Aluminium isopropoxide, TEAOH, and DI water were mixed and stirred for an hour at room temperature to form a homogeneous mixture. Phosphoric acid was added dropwise into the stirring solution. The resulting precursor solution was stirred again for 2 hours before heated hydrothermally at 150°C for 20 hours. The synthesized particles were centrifuged at 6000 rpm for 10 minutes to collect the seeds and washed with DI water. The resulting crystal was dried at 50 °C for overnight.

2.3. Functionalization of zeolite AlPO-18

The synthesized zeolite AlPO-18 powder was dried overnight at 50 °C before functionalization. For functionalization, 2 g of zeolite AlPO-18 powder was uniformly dispersed into 50 mL of toluene. Then, 4 mL of APTES was added dropwise to the resultant mixture and refluxed at 110 °C for 4 hours. After the reflux process, the mixture was filtered and rinsed with toluene and ethanol absolute in order to remove the unreacted APTES. The washed particles were dried at 50 °C overnight. AlPO-18 that was functionalized by the silane group was denoted as NH_2-AlPO-18 in the current project.

2.4. Characterization of zeolite AlPO-18 and NH_2-AlPO-18

XRD (X'Pert^3 Powder & Empyrean, PANalytical) was used to study the crystallinity of zeolite AlPO-18 and NH_2-AlPO-18. The analysis was carried out at an accelerating voltage of 40 kV and current of 40 mA and by using Cu Kα radiation at 2θ in the range of 5^o - 45^o with a step size of 0.05^o. Fourier Transform Infrared-Attenuated Total Reflection, FTIR-ATR (Perkin Elmer, Frontier) was used to identify the functional groups and chemical bondings presence in the zeolite AlPO-18 and NH_2-AlPO-18. The analysis was carried out with a wavelength of 4000 cm^{-1} to 400 cm^{-1}. Thermogravimetric Analysis, TGA (Perkin Elmer, STA 6000) was used to study the thermal stability of zeolite AlPO-18 and NH_2-AlPO-18 based on the weight loss of the sample due to change in temperature over time. The samples were heated from 30 °C to 800 °C at a constant heating rate of 10 ^oC/min under N_2 atmosphere. Field Emission Scanning Electron Microscopy, FESEM (Zeiss Supra 55VP) was used to study the morphology of the zeolite AlPO-18 and NH_2-AlPO-18. Energy-Dispersive spectroscopy (EDX) was used to identify the elemental compositions of zeolite AlPO-18 and NH_2-AlPO-18.

3. Results and discussions

3.1. Crystallinity analysis of zeolite AlPO-18 and NH_2-AlPO-18

The XRD pattern of the calcined zeolite AlPO-18 and NH_2-AlPO-18 are illustrated in figure 2. From figure 2(a), it can be observed that the XRD pattern display the peaks at two theta of 9.6°, 12.8°, 16.8°, 21°, 23.6°, 26.2°, and 32.0°. All the XRD peaks of the synthesized zeolite AlPO-18 were similar to the XRD patterns reported in the literature previously [32–35]. The results obtained prove that zeolite AlPO-18 was successfully synthesized. According to Carreon *et al.* [35], the XRD pattern exhibit broad and less intense peaks due to the presence of amorphous regions and/or there is a high degree of structural disorder in the synthesized zeolite AlPO-18 framework.

From figure 2(b), it can be seen that the XRD pattern of NH_2-AlPO-18 was almost similar to the zeolite AlPO-18 peaks. This implies the zeolite structure was not affected by the functionalization of aminosilane on the zeolite surface. Despite that, the intensity of NH_2-AlPO-18 peak was lower compared to the zeolite AlPO-18 patterns. This could be due to the pore filling effect, where the pore surface of zeolite AlPO-18 is probably covered by APTES groups. Thus, it affects the crystallinity of the sample by causing a slight decrement in the peak crystallinity [36, 37].

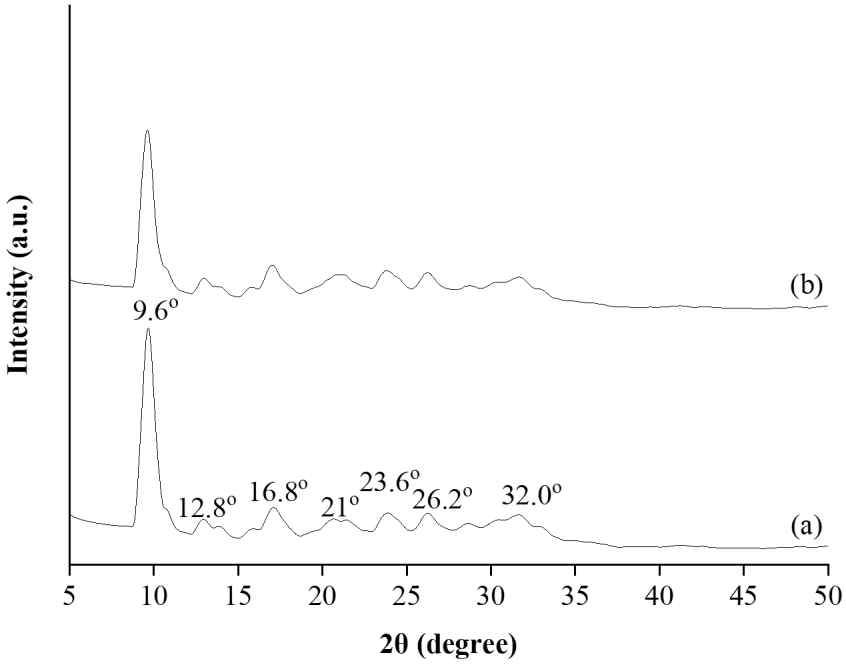

Figure 2. XRD patterns of (a) zeolite AlPO-18 and (b) NH_2-AlPO-18.

3.2. Spectroscopic analysis of zeolite AlPO-18 and NH_2-AlPO-18

Figure 3 and figure 4 shows the FTIR spectra of calcined zeolite AlPO-18 and NH_2-AlPO-18 in the region of 4000-400 cm^{-1}. FTIR was used to identify the functional group and type of bonding present in zeolite AlPO-18 and zeolite NH_2-AlPO-18. From figure 3(a), it can be seen that the FTIR spectra exhibits the bands around 3500 cm^{-1}, 1640 cm^{-1}, 1100 cm^{-1}, 600 cm^{-1} and 500 cm^{-1}. All these bands are the typical zeolite AlPO-18 peaks that are in good agreement with the literature reported previously [34, 38, 39].

The broad absorption band around 3800-3200 cm^{-1} was attributed to H- bonded Al-OH and P-OH groups [34, 40–42]. Besides that, the band around 1700-1600 cm^{-1} attributed to the interlayer bending vibration of physically adsorbed water molecules [43–45]. P-O stretching and bending were ascribed to the bands observed in the region of 1200-1000 cm^{-1} and about 500 cm^{-1}, respectively [43, 46]. The presence of double 8-rings framework in the zeolite AlPO-18 was linked to a small intensity band formed around 650 cm^{-1} [42, 47, 48].

From figure 3(b) and figure 4(b), it can be seen that the FTIR spectra of NH_2-AlPO-18 was almost similar to the zeolite AlPO-18 spectra with a few additional bands around 1500 ~ 1300 cm^{-1} and 1560 cm^{-1}. Compared to zeolite AlPO-18, the zeolite NH_2 - AlPO-18 showed a broader band at the frequency of 3800-3200 cm^{-1}, where the band assigned to N-H stretching of a primary amine overlaps with the O-H stretching of hydroxyl group, indicating the presence of aminosilane in the sample [15, 49]. Besides that, Si-CH_2 and Si-CH_3 stretching vibrations of the aminosilane were also apparent around 1500-1300 cm^{-1} in NH_2-AlPO-18 [12, 40, 50]. Moreover, the presence of an absorption peak at 1560 cm^{-1}, which indicates N-H bending of the amine, was also absent in zeolite AlPO-18 [15].

The type of bonding represented by each of the peak presence in zeolite AlPO-18 and NH_2-AlPO-18 spectra were summarised in table 1.

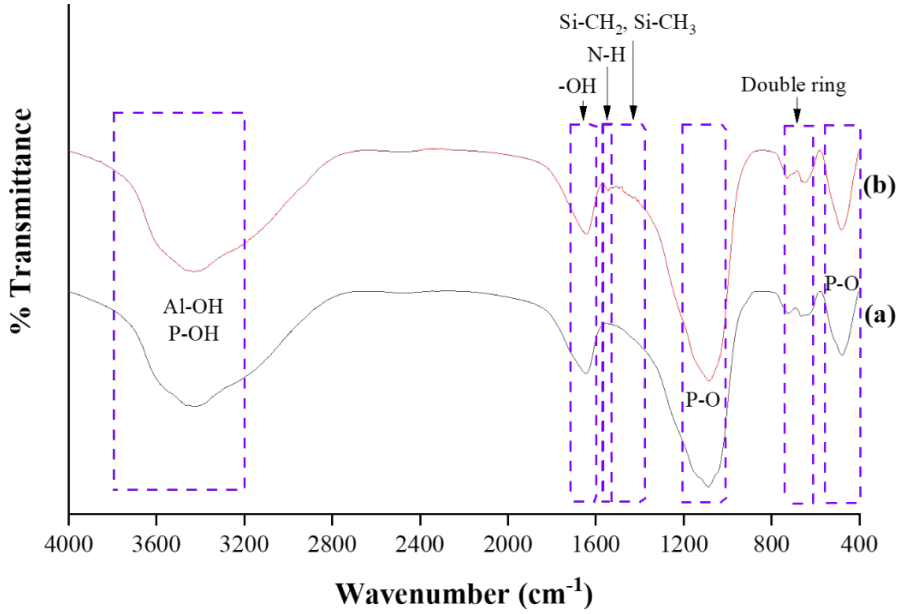

Figure 3. FT-IR spectra of (a) zeolite AlPO-18 and (b) NH_2-AlPO-18.

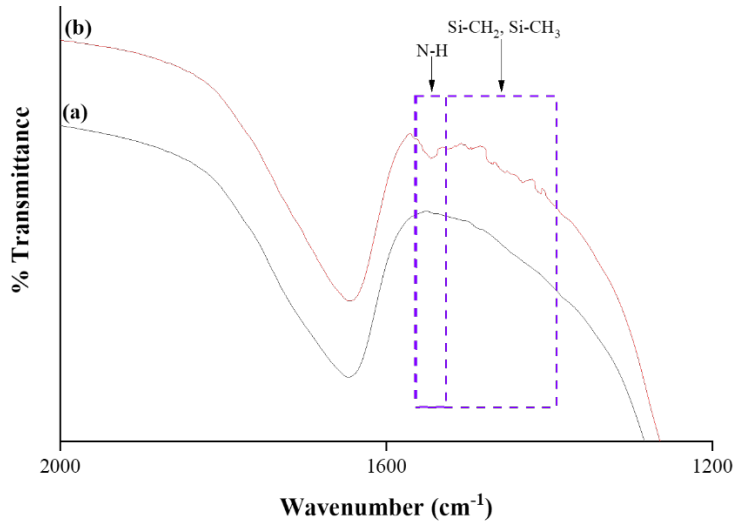

Figure 4. FT-IR spectra of (a) zeolite AlPO-18 and (b) NH_2-AlPO-18 in the range 2000-1200 cm^{-1}.

Table 1. Type of bonding shown in the FTIR spectra of zeolite AlPO-18 and NH_2-AlPO-18.

Wavenumber (cm^{-1})	Type of bonding
3800 ~ 3200	–OH stretching of hydroxyl group
3434#	N–H stretching of primary amine
1640	–OH bending of hydroxyl group
1560#	N–H bending of primary amine
1500 ~ 1300#	Si–CH_2 and Si–CH_3 stretching of aminosilane
1200 ~ 1000	P–O stretching
650 ~ 500	Double 8-rings framework
~ 500	P–O bending

#*Attributed to silane groups*

3.3. Thermal analysis of zeolite AlPO-18 and NH_2-AlPO-18

Figure 5 illustrates the TGA diagram of zeolite AlPO-18 and NH_2-AlPO-18. TGA profile shows the percentage of weight loss of the zeolite AlPO-18 and NH_2-AlPO-18 as a function of time.

From the figure 5, it can be observed that zeolite AlPO-18 exhibits a single-stage decomposition process in the temperature range of 30-200 ^oC. Whereas, NH_2-AlPO-18 shows a two-stage decomposition at the temperature ranged from 30-200 ^oC and 200-800 ^oC. In figure 5(a), the TGA profile of zeolite AlPO-18 shows a significant weight loss of 24.72% below 200 ^oC, which was almost similar to the TGA profile reported in the literature [51, 52]. This weight loss was ascribed to the removal of physiosorbed water molecules within the zeolite pores [51, 53, 54]. After 200 ^oC, there is no obvious mass variation of zeolite AlPO-18 up to 800 ^oC, which clarifies that zeolite AlPO-18 has good thermal stability.

The TGA profile of NH_2-AlPO-18 in figure 5(b) illustrates the first-stage decomposition with a weight loss of 19.52% at the temperature range of 30-200 ^oC. The thermal decomposition rate of NH_2-AlPO-18 was lower compared to zeolite AlPO-18. This justifies the attachment of APTES silane groups on the hydroxyl groups (-OH) of zeolite AlPO-18 during the grafting process [55–57]. Thus, it can be concluded that the small weight loss in NH_2-AlPO-18 is because of less -OH group presence in the NH_2-AlPO-18 sample. The second-stage decomposition of NH_2-AlPO-18 with a weight loss of 3.94 % occurs at the temperature range 200-800 ^oC. This weight loss was attributed to gradual organic volatilization-decomposition of propyl chain in APTES molecule [22, 58–61]. The thermal properties of zeolite AlPO-18 and NH_2-AlPO-18 are summarized in table 2.

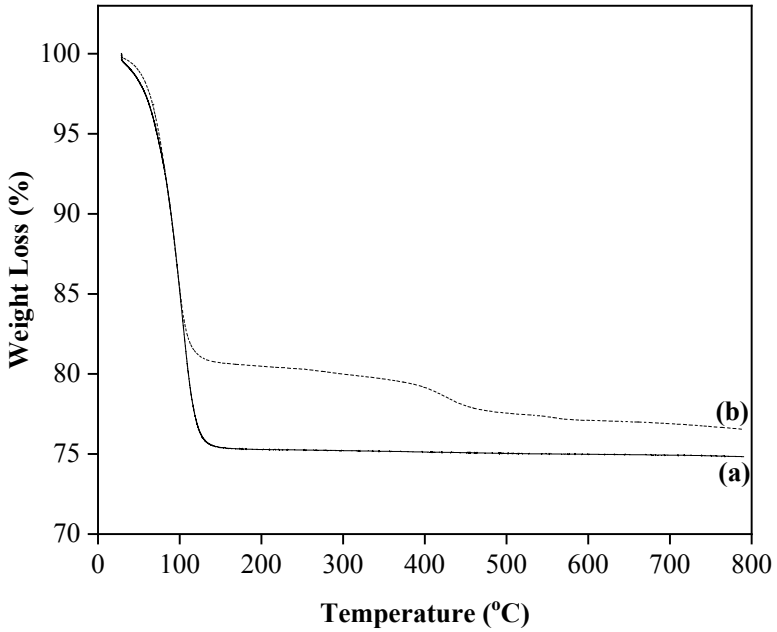

Figure 5. TGA diagram of (a) zeolite AlPO-18 and (b) NH_2-AlPO-18.

Table 2. Weight loss of zeolite AlPO-18 and NH_2-AlPO-18 at different temperatures.

Stages of weight loss	Weight loss (%)	
	Zeolite AlPO-18	**NH_2-AlPO-18**
Desorption of adsorbed water (30 – 200°C)	24.72	19.52
Decomposition of APTES (200 – 800°C)	-	3.94
Total	24.72	23.46

3.4. Morphological analysis of zeolite AlPO-18 and NH_2-AlPO-18

Figure 6(a) and (b) shows the FESEM images of zeolite AlPO-18 and NH_2-AlPO-18 at a magnification of 20kX respectively. FESEM was used to examine the morphology of the zeolite AlPO-18 and NH_2-AlPO-18.

The FESEM images in figure 6(a) show a thin elongated plate-like structure of zeolite AlPO-18. The morphology obtained is the typical zeolite AlPO-18 structure that looks similar to the literature reported previously [30, 51]. However, the morphology of the samples displays particle aggregates. Besides that, from figure 6(b), it can be observed that the morphology of NH_2-AlPO-18 was similar to that of zeolite AlPO-18 even after functionalization on the surface of zeolite AlPO-18. This shows that the functionalization of aminosilane on the zeolite surface had no effect on the zeolite structure.

Moreover, EDX spectroscopy was used to identify the composition of the element presence in zeolite AlPO-18 and NH_2-AlPO-18. To ensure the consistency of the composition, five trials of the analysis were carried out on the samples. The elemental composition of the samples is summarized in table 3. Aluminium (Al), Phosphorus (P), and Oxygen (O) are the main elements of zeolite AlPO-18 whereas Nitrogen (N) is the main element in APTES. Thus, the presence of N in the EDX of NH_2-AlPO-18 sample proves the presence of APTES in the sample.

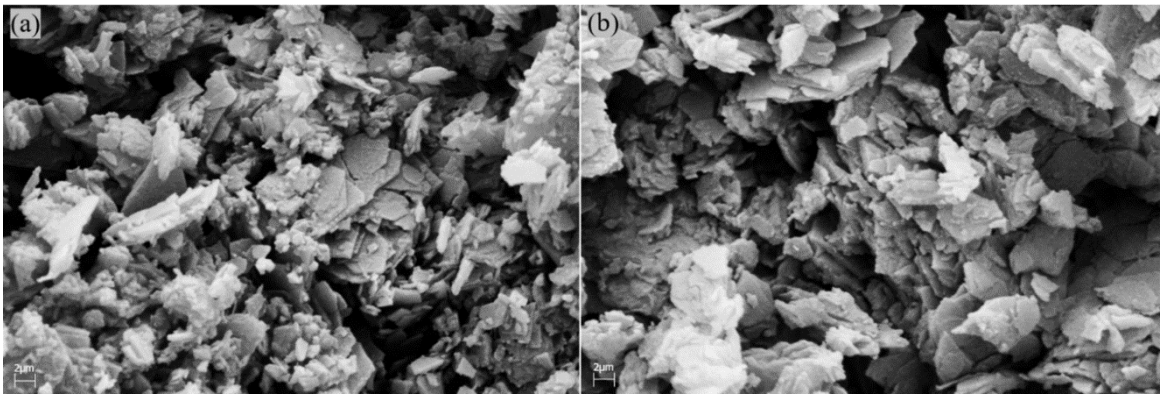

Figure 6. FESEM images of (a) zeolite AlPO-18 and (b) NH_2-AlPO-18.

Table 3. EDX of zeolite AlPO-18 and NH_2-AlPO-18.

Samples	Weight composition (Weight %)				
	Al	**P**	**O**	**N**	**Total**
Zeolite AlPO-18	19.42	25.52	55.06	Not detected	100.00
NH_2-AlPO-18	18.39	23.75	54.84	3.02	100.00

4. Conclusion

In the current project, the effect of aminosilane functionalization on zeolite AlPO-18 was investigated. The XRD pattern of NH_2-AlPO-18 was comparable to that of zeolite AlPO-18, although the peak intensity was lower than that of zeolite AlPO-18. The existence of N-H stretching and bending vibration bands of aminosilane was observed in the FTIR spectra of NH_2-AlPO-18 sample. According to FESEM analysis, even after functionalization, the morphology of NH_2-AlPO-18 was similar to that of zeolite AlPO-18, demonstrating that aminosilane functionalization has no effect on zeolite structure. Furthermore, EDX confirms the existence of 3.02 percent element N in the NH_2-AlPO-18 sample. All of the characterizations revealed the presence of APTES in the NH_2-AlPO-18 sample. The obtained NH_2-AlPO-18 can be used widely in industrial applications such as molecular separation, adsorption, and catalysis. For future research, the NH_2-AlPO-18 can be potentially used as filler for CO_2/CH_4 gas separation. Besides that, the effect of various types of silane coupling agents such as (3-aminopropyl) dimethylethoxysilane (APDMES) and (3-aminopropyl) methyldiethoxysilane (APMDES) on the zeolite properties can also be investigated.

Acknowledgments

The authors would like to express gratitude to financial support from Fundamental Research Grant Scheme (FRGS) Ref: FRGS/1/2020/TK0/UTP/02/28 (Cost center: 015MA0-123) from the Ministry of Higher Education Malaysia (MOHE). This work was also supported by Universiti Teknologi PETRONAS, Institute Contaminant Management UTP, CO_2 Research Centre (CO_2RES) UTP.

References

[1] Prech J, Pizarro P, Serrano D P and Cejka J 2018 From 3d to 2d zeolite catalytic materials *Chem. Soc. Rev.* **47** 8263–306
[2] Wu T, Tanaka K, Chen X, Kumakiri I and Kita H 2018 Synthesis and gas permeation properties of aei zeolite membranes by dipea as a template *Membrane* **43** 67–73
[3] Feng C, Khulbe K C, Matsuura T, Farnood R and Ismail A F 2015 Recent progress in zeolite/zeotype membranes *J. Membr. Sci. Res.* **1** 49–72
[4] Database of zeolite structures [Internet] Available from: http://www.iza-structure.org/databases/
[5] Huang L, Xiao H and Ni Y 2006 Cationic-modified microporous zeolites/anionic polymer system for simultaneous removal of dissolved and colloidal substances from wastewater *Sep. Purif. Technol.* **49** 264–70
[6] Kuwahara Y, Kamegawa T, Mori K, Matsumura Y and Yamashita H 2009 Fabrication of hydrophobic zeolites using triethoxyfluorosilane and their application for photocatalytic degradation of acetaldehyde *Top. Catal.* **52** 643–8
[7] Smaïhi M, Gavilan E, Durand J O and Valtchev V P 2004 Colloidal functionalized calcined zeolite nanocrystals *J. Mater. Chem.* **14** 1347–51
[8] Zhang X, Lai E S M, Martin-Aranda R and Yeung K L 2004 An investigation of knoevenagel condensation reaction in microreactors using a new zeolite catalyst *Appl. Catal. A-Gen.* **261** 109–18
[9] Zhang X Y, Wang Q C, Zhang S Q, Sun X J and Zhang Z S 2009 Stabilization/solidification (s/s) of mercury-contaminated hazardous wastes using thiol-functionalized zeolite and portland cement *J. Hazard. Mater.* **168** 1575–80
[10] Chen X Y, Nik O G, Rodrigue D and Kaliaguine S 2012 Mixed matrix membranes of aminosilanes grafted fau/emt zeolite and cross-linked polyimide for co2/ch4 separation *Polymer* **53** 3269–80
[11] Chua L K, Jusoh N and Yeong Y K 2015 Fabrication of sapo-34 and silane-modified sapo-34/polyimide mixed matrix membranes for co2/ch4 separation *J. Appl. Sci. Agric.* **10** 215–21
[12] Amooghin A E, Omidkhah M and Kargari A 2015 The effects of aminosilane grafting on nay zeolite–matrimid®5218 mixed matrix membranes for co2/ch4 separation *J. Membr. Sci.* **490** 364–79

[13] Nik O G, Chen X Y and Kaliaguine S 2011 Amine-functionalized zeolite fau/emt-polyimide mixed matrix membranes for co_2/ch_4 separation *J. Membr. Sci.* **379** 468–78
[14] Pechar T W, Tsapatsis M, Marand E and Davis R 2002 Preparation and characterization of a glassy fluorinated polyimide zeolite-mixed matrix membrane *Desalination* **146** 3–9
[15] Sanaeepur H, Kargari A and Nasernejad B 2014 Aminosilane-functionalization of a nanoporous y-type zeolite for application in a cellulose acetate based mixed matrix membrane for co_2 separation *RSC Adv.* **4** 63966–76
[16] Junaidi M U M, Khoo C P, Leo C P and Ahmad A L 2014 The effects of solvents on the modification of sapo-34 zeolite using 3-aminopropyl trimethoxy silane for the preparation of asymmetric polysulfone mixed matrix membrane in the application of co_2 separation *Microporous Mesoporous Mater.* **192** 52–9
[17] Kumudinie C 2001 Polymer-ceramic nanocomposites: Interfacial bonding agents *Encyclopedia of Materials: Science and Technology* 7574–7
[18] Ahmad N N R, Mukhtar H, Mohshim D F, Nasir R and Man Z 2016 Surface modification in inorganic filler of mixed matrix membrane for enhancing the gas separation performance *Rev. Chem. Eng.* **32** 1–20
[19] Chung T S, Jiang L Y, Li Y and Kulprathipanja S 2007 Mixed matrix membranes (mmms) comprising organic polymers with dispersed inorganic fillers for gas separation *Prog. Polym. Sci.* **32** 483–507
[20] Liu X M, Thomason J L and Jones F R: Taylor & Francis Group; 2009 Xps and afm study of the structure of hydrolysed aminosilane on e-glass surfaces In: Mittal KL, editor *Silanes and other coupling agents* 5 Boston p 39–50
[21] Smith E A C and Wei 2008 How to prevent the loss of surface functionality derived from aminosilanes *Langmuir* **2008** 12405–9
[22] Berktas I, Ghafar A N, Fontana P, Caputcu A, Menceloglu Y and Okan B S 2020 Facile synthesis of graphene from waste tire/silica hybrid additives and optimization study for the fabrication of thermally enhanced cement grouts *Molecules* **25** 1–15
[23] Liu Y, Zhang S, He Y, Chen C, Zhang C, Xie P, Zhong F, Li H, Chen J and Li Z 2021 Aptes modification of molybdenum disulfide to improve the corrosion resistance of waterborne epoxy coating *Coatings* **11** 1–13
[24] Lo X C, Li J Y, Lee M T and Yao D J 2020 Frequency shift of a sh-saw biosensor with glutaraldehyde and 3-aminopropyltriethoxysilane functionalized films for detection of epidermal growth factor *Biosensors (Basel)* **10** 1–12
[25] Wang J 2020 A simple, rapid and low-cost 3-aminopropyltriethoxysilane (aptes) based surface plasmon resonance sensor for tnt explosive detection *Anal. Sci.* 1–17
[26] Yang J, Liao M, Hong G, Dai S, Shen J, Xie H and Chen C 2020 Effect of aptes- or mpts-conditioned nanozirconia fillers on mechanical properties of bis-gma-based resin composites *ACS Omega* **5** 3254–50
[27] Zhang B, Wang Y, Zhang J, Qiao S, Fan Z, Wan J and Chen K 2020 Well-defined 3-aminopropyltriethoxysilane functionalized magnetite nanoparticles and their adsorption performance for partially hydrolyzed polyacrylamide from aqueous solution *Colloids and Surfaces A: Physicochemical and Engineering Aspects* **586** 1–31
[28] Soria S, Berneschi S, Barucci A, Cosci A, Farnesi D, Conti G N, Pelli S and Righinia G C: Jenny Stanford; 2019 Biomedical sensing applications of microspherical resonators In: Righini GC, editor *Glass microand nanospheres : Physics and applications* USA p 165–201
[29] Rao X, Tatoulian M, Guyon C, Ognier S, Chu C and Abou Hassan A 2019 A comparison study of functional groups (amine vs. Thiol) for immobilizing aunps on zeolite surface *Nanomaterials (Basel)* **9** 1–14
[30] Wang B, Gao F, Zhang F, Xing W and Zhou R 2019 Highly permeable and oriented alpo-18 membranes prepared using directly synthesized nanosheets for co_2/ch_4 separation *J. Mater. Chem. A.* **7** 13164–72

[31] Zong Z, Elsaidi S K, Thallapally P K and Carreon M A 2017 Highly permeable alpo-18 membranes for n_2/ch_4 separation *Ind. Eng. Chem. Res.* **56** 4113–8
[32] Vilaseca M, Mintova S, Valtchev V, Metzger T H and Bein T 2003 Synthesis of colloidal alpo4-18 crystals and their use for supported film growth *J. Mater. Chem.* **13** 1526–8
[33] Wu T, Wang B, Lu Z, Zhou R and Chen X 2014 Alumina-supported alpo-18 membranes for co_2/ch_4 separation *J. Membr. Sci.* **471** 338–46
[34] Chen J, Thomas J M, Wright P A and Townsend R P 1994 Silicoaluminophosphate number eighteen (sapo- 18): A new microporous solid acid catalyst *Catal. Lett.* **28** 241–8
[35] Carreon M L, Li S and Carreon M A 2012 Alpo-18 membranes for co2/ch4 separation *Chem Commun (Camb)* **48** 2310–2
[36] Babaei M, Anbia M and Kazemipour M 2017 Improving co_2 adsorption with new amine-functionalized y-type zeolite *J. Adv. Environ. Health. Res.* **5** 70–7
[37] Kim S, Ida J, Guliants V V and Lin J Y S 2005 Tailoring pore properties of mcm-48 silica for selective adsorption of co_2 *J. Phys. Chem. B* **109** 6287–93
[38] Peng L, Li J, Yu J, Li G, Fang Q and Xu R 2005 [h3n(ch2)4nh3]2[al4(c2o4)(h2po4)2(po4)4]·4[h2o]: A new layered aluminum phosphate-oxalate *Journal of Solid State Chemistry* **178** 2686–91
[39] Preethi M E L, Umasankari A, C.H. R, Palanichamy M, Sivakumar T and Pandurangan A 2018 Selective oxidation of cyclohexane to ka oil over ce-alpo-18 molecular sieves *Int. J. Eng. Technol.* **7** 352–4
[40] Gianotti E, Oliveira E C, Dellarocca V, Coluccia S, Pastore H O and Marchese L 2002 Meso-alpo prepared by thermal decomposition of the organic-inorganic composite: A ftir study *Nanoporous materials iii, proceedings of the 3rd international symposium on nanoporous materials* Studies in surface science and catalysis 417–22
[41] Martis M In situ and ex situ characterization studies of transition metal containing nanoporous catalysts: University College London; 2011
[42] Byarappa K and Kumar S B V 2007 Characterization of zeolites by infrared spectroscopy *Asian J. Chem.* **19** 4933–5
[43] Boonchom B, Youngme S, Srithanratana T and Danvirutai C 2008 Synthesis of $alpo_4$ and kinetics of thermal decomposition of $alpo_4 \cdot h_2o\text{-}h_4$ precursor *J. Therm. Anal. Calorim.* **91** 511–6
[44] Popescu S C, Thomson S and Howe R F 2001 Microspectroscopic studies of template interactions in $alpo_4$-5 and sapo-5 crystals *Phys. Chem. Chem. Phys.* **3** 111–8
[45] Ng E P, Awala H, Komaty S and Mintova S 2019 Microwave-green synthesis of alpo-n and sapo-n (n = 5 and 18) nanosized crystals and their assembly in layers *Microporous Mesoporous Mater.* **280** 256–63
[46] Mustafa S, Javid M and Zaman M I 2006 Effect of activation on the sorption properties of $alpo_4$ *Sep. Sci. Technol.* **41** 3467–84
[47] Venkatathri N 2005 Synthesis and characterization of alpo4-21 from aqueous and non-aqueous systems *Bulletin of the Catalysis Society of India* **4** 18–27
[48] Zhao D, Zhang Y, Li Z, Wang Y and Yu J 2017 Synthesis of sapo-18/34 intergrowth zeolites and their enhanced stability for dimethyl ether to olefins *RSC Adv.* **7** 939–46
[49] Cheng F, Sajedin S M, Kelly S M, Lee A F and Kornherr A 2015 Uv-stable paper coated with aptes-modified p_{25} tio_2 nanoparticles *Elsevier* 1–18
[50] Ismail A, Kusworo T and Mustafa A 2008 Enhanced gas permeation performance of polyethersulfone mixed matrix hollow fiber membranes using novel dynasylan ameo silane agent *J. Membr. Sci.* **319** 306–12
[51] van Heyden H, Mintova S and Bein T 2006 Alpo-18 nanocrystals synthesized under microwave irradiation *J. Mater. Chem.* **16** 514–8
[52] Tosheva L N, Ng E P, Mintova S, Holzl M, Metzger T H and Doyle A M 2008 Alpo4-18 seed layers and films by secondary growth *Chem. Mater.* **2008** 5721–6

[53] Chen C, Feng B, Hu S, Zhang Y, Li S, Gao L, Zhang X and Yu K 2018 Control of aluminum phosphate coating on mullite fibers by surface modification with polyethylenimine *Ceramics International* **44** 216–24
[54] Karka S, Kodukula S, Nandury S V and Pal U 2019 Polyethylenimine-modified zeolite 13x for co_2 capture: Adsorption and kinetic studies *ACS Omega* **4** 16441–9
[55] Hanim S A M, Malek N A N N and Ibrahim Z 2016 Amine-functionalized, silver-exchanged zeolite nay: Preparation, characterization and antibacterial activity *Appl. Surf. Sci.* **360** 121–30
[56] Li P, Zhang Y, Zuo Y, Lu J, Yuan G and Wu Y 2019 Comparative study of organic and inorganic modification of chinese fir wood based on the respiratory impregnation method
[57] Wang J, Stevens L A, Drage T C and Wood J 2012 Preparation and co2 adsorption of amine modified mg–al ldh via exfoliation route *Chemical Engineering Science* **68** 424–31
[58] Abdi J, Vossoughi M, Mahmoodi N M and Alemzadeh I 2017 Synthesis of amine-modified zeolitic imidazolate framework-8, ultrasound-assisted dye removal and modeling *Ultrason. Sonochem.* **39** 550–64
[59] Bakdash R S, Aljundi I H, Basheer C and Abdulazeez I 2020 Rice husk derived aminated silica for the efficient adsorption of different gases *Sci Rep* **10** 19526
[60] Maity D, Chandrasekharan P, Feng S S and Jun D 2010 Synthesis and studies of aptes functionalized magnetite nanoparticles International Conference on Nanoscience and Nanotechnology (ICONN) 94–7
[61] Sehlleier Y H, Abdali A, Schnurre S M, Wiggers H and Schulz C 2014 Surface functionalization of microwave plasma-synthesized silica nanoparticles for enhancing the stability of dispersions *Journal of Nanoparticle Research* **16** 1–11